

Dynamic Response of FGM Plates Under Blast Load

Reza Azarafza^{*}, Puya Pirali, Ali Davar, Majid Ghadimi

Faculty of Materials and Manufacturing Technologies,

Malek Ashtar University of Technology, Tehran, Iran

E-mail: azarmut@mut.ac.ir, ppirali@mut.ac.ir, davar78@gmail.com, ghadimi_m2@yahoo.com

^{*}Corresponding author

Received: 9 January 2021, Revised: 2 April 2021, Accepted: 9 April 2021

Abstract: The present study investigates the deformation of FGM plates under blast load. Hamilton's principle is used to obtain the dynamic Equations. The two constituent phases, ceramic and metal, vary across the wall thickness according to a prescribed power law. Boundary conditions are assumed to be Simply Supported (SS). The type of explosive loading considered is a free in-air spherical air burst and creates a spherical shock wave that travels radially outward in all directions. For the pressure time of the explosion loading, Friedlander's exponential relation has been used. In order to determine the response analytically, the stress potential field function is considered. Using the Galerkin method, the final Equations are obtained as nonlinear and nonhomogeneous second-order differential Equations. The effect of temperature including thermal stress resultants and different parameters on the dynamic response have been investigated. Results have been compared with references and validated. Results showed that the amplitude of the center point deflection of the FGM plate is less than the pure metal plates when exposed to blast load, by increasing the volumetric index percentage of FGM, center point deflection is increased and in the FGM plates, deformation of symmetrical plates is smaller than the asymmetric plates. Also by applying the damping coefficient of the FGM plates, the amplitude of center point deflection is reduced, and by increasing the aspect ratio of the FGM plate, its center point deflection against explosion waves is reduced and by considering the effects of thermal resultant forces and moments, center point deflection is increased.

Keywords: Dynamic Response, Explosive Loading, Functional Graded Materials, Rectangular FGM Plates

Biographical notes: **Reza Azarafza** is an Associate Professor of Mechanical Engineering at Malek Ashtar University of Technology, Tehran, Iran. His current research focuses on composite structures, plates and shell analysis, and vibrations. **Puya Pirali** is an Assistant Professor at the Department of Mechanical Engineering, at Malek Ashtar University of Technology, Tehran, Iran. His current research focuses on plates and shell analysis. **Ali Davar** is currently an Assistant Professor at the Department of Mechanical Engineering, at Malek Ashtar University, Tehran, Iran. His current research interest includes composite structures. **Majid Ghadimi** is currently a PhD student at Malek Ashtar University and his main research interests are composite structures and Modal Analysis.

Research paper

COPYRIGHTS

© 2023 by the authors. Licensee Islamic Azad University Isfahan Branch. This article is an open access article distributed under the terms and conditions of the Creative Commons Attribution 4.0 International (CC BY 4.0)

(<https://creativecommons.org/licenses/by/4.0/>)



1 INTRODUCTION

Increasing the knowledge of scientific and industrial communities always has been a factor in improving technology and achieving superior technology. In this regard, the use of new materials to achieve specific functional properties always have been a consideration of engineering researchers. Functionally graded Material (FGM) is a kind of modern material that has been widely used in recent years. Extensive research has been conducted to produce the FGM in order to resist high temperature and thermal shock for use in the body of spacecraft and nuclear power plants. FGMs are a kind of composite materials that are heterogeneous in terms of infrastructure, and the volume fraction of its constituent material is a function of the spatial position in each body, so that, in accordance with volume fraction, the other mechanical properties are also exhibiting continually gradual changes along the thickness from one plane to another. This feature of these materials not only increases their resistance to mechanical loadings but also makes them tolerable in extreme temperature gradient environments. The common type of this material is the combination of ceramic and metal, in which case it has a metal face and the other face is ceramic, and mechanical properties change continually from metal to ceramic through the thickness [1].

Recently, more attention has been paid to the design and development of explosion-resistant structures. As in most countries, extensive studies have been done on the reaction of structures, buildings, facilities, and equipment against explosions caused by explosive materials. Therefore, considering the remarkable characteristics of FGM materials of ceramic-metal based combination, in carrying loads such as explosion and penetration, investigating and understanding the behavior and response of these materials under various dynamic loads such as the explosion wave has been attractive to the researchers.

So far, extensive research has been done to study the mechanical effects of explosion on plates made of FGM materials, which can be mentioned below. Turkmen and Mecitoglu [2] compared the results of experimental tests and numerical solutions with the finite element method for a composite plate with reinforced layers under explosive load, and the effect of reinforcements and applied load on the dynamic response of the plate has been studied. Chi and Chung [3] have studied the mechanical behaviour of an elastic rectangular plate supported on the FGM bed exposed to transversal loading with SS boundary conditions. Alibeigloo [4] has studied the three-dimensional thermoelastic analysis of FGM rectangular plates with small deformation on SS boundary conditions. In this study, the thermoelastic

properties of the plate change with exponential function in the thickness direction. Tung and Duc [5] studied the nonlinear analysis of stability for functionally graded plates under mechanical and thermal loads. Hause [6] has investigated the deflection of the functionally graded plates under the influence of the explosion theoretically. The theory of classic plates (CPT) has been used and plates have been exposed to a Friedlander explosive loading. Aksoylar et al. [7] investigated the nonlinear transient analysis of FGM and FML composite plates under non-destructive explosive loads using experimental and FE methods.

Sreenivas et al. [8] studied and investigated the transient dynamic response of functionally graded materials. Goudarzi and Zamani [9] have investigated the maximum deflection of circular plates under the effect of uniform and nonuniform shock waves due to explosion by experimental and numerical analysis. Duong and Duc [10] considered the evaluation of the elastic properties and thermal expansion coefficient of composites reinforced by randomly distributed spherical particles with negative Poisson ratios. Duc et al. [11] presented the nonlinear dynamic response and vibration of imperfect shear deformable functionally graded plates subjected to blast and thermal loads. Duc et al. [12] presented the nonlinear dynamic and vibration of the S-FGM shallow spherical shells resting on elastic foundations including temperature effects. Cong et al. [13] investigated the nonlinear vibration and dynamic response of ES-FGM plates using third-order shear deformation theory (TSDT).

Hajlaoui et al. [14] presented the nonlinear dynamics analysis of FGM shell structures with a higher order shear strain enhanced solid-shell element. Tong et al. [15] studied the thermo-mechanical buckling and post-buckling of cylindrical shells with functionally graded coatings reinforced by stringers. Duc et al. [16] presented the nonlinear dynamic response of functionally graded porous plates on elastic foundations subjected to thermal and mechanical loads. Cong and Duc [17] studied analytical solutions for the nonlinear dynamic response of ES-FGM plates under blast load. Kim et al. [18] studied the nonlinear vibration and dynamic buckling of eccentrically oblique stiffened FGM plates resting on elastic foundations in a thermal environment. Duc et al. [19] presented the free vibration and nonlinear dynamic response of imperfect nanocomposite FG-CNTRC double-curved shallow shells in a thermal environment.

The main goal of this paper is to calculate the dynamic response of FGM plates under explosive load by considering the thermal forces and moments. Studying the effect of thermal forces and moments on the response of FGM plate is one of the innovations and advantages of this research that less has been studied in the previous research and the literature. Also, the effect of the

damping coefficient, power law index of FGM plate, aspect ratio ($L1/L2$) of FGM plate, and symmetric and asymmetric FGM plate on dynamic response have been investigated.

2 GOVERNING EQUATIONS

2.1. Mechanical Properties of FGM Material

As shown in “Fig. 1”, a rectangular FGM plate with dimensions $L1$ and $L2$ and thickness h is in Cartesian coordinates, so that the origin of the coordinate system (x, y, z) is located at the middle surface of the plate.

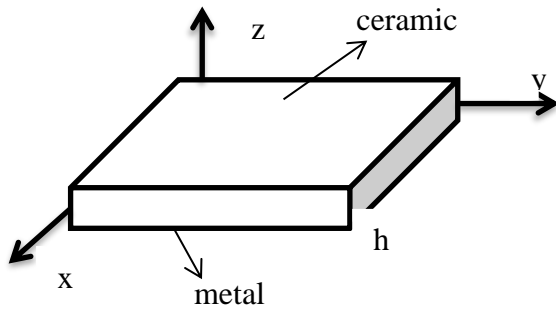


Fig. 1 Geometric characteristic of FG plate.

If V_m and V_c are the volume fractions of ceramic and metal in the FGM, respectively, then the relation of each mechanical property related to the volume fractions will be as follows [20]:

$$P_f(z) = P_m V_m(z) + P_c V_c(z) \quad (1)$$

As P_m and P_c are, respectively, metal and ceramic properties in the FGM, therefore, with respect to the above relations, the properties of a FGM material such as modulus of elasticity, linear coefficient of expansion, shear modulus, or density can be obtained as:

$$P_f(z) = (P_c - P_m) V_c(z) + P_m \quad (2)$$

Two cases for grading and gradual changes of ceramic and metal phases along the thickness of FG plates can be considered:

Symmetrical case: The ceramic and metal phase elements are changed symmetrically in the thickness direction of plate, so that both outer surfaces of the plate are completely ceramic and the middle surface of the plate is full metal. In this case, the volume fractions of ceramic $V_c(z)$ is expressed in the form of Equation (3) [6]:

$$V_c(z) = \left(\frac{z}{h/2} \right)^N \left(\frac{1 + \text{sgn}(z)}{2} \right) + \left(\frac{-z}{h/2} \right)^N \left(\frac{1 - \text{sgn}(z)}{2} \right) \quad (3)$$

In the above Equation, N is the volumetric percentage index of the material FGM, h is the thickness of the plate and z is the coordinates perpendicular to the middle surface along the thickness direction.

Asymmetrical case: Ceramic and metal phase elements change asymmetrically in the thickness direction of the plate, the upper surface of the plate is full ceramic and the bottom surface of the plate is full metal. In this case, as in “Fig. 1”, the bottom of the plate is completely metallic and its upper surface is completely ceramic and between these two surfaces will be a combination of ceramic and metal. In this case, the volume fraction of ceramic $V_c(z)$ is expressed in the form of Equation (4) [6]:

$$V_c(z) = \left(\frac{2z+h}{2h} \right)^N \quad (4)$$

Regarding the function of FGM materials in high-temperature environments, according to Reddy [1], the mechanical properties of its constituents have significant changes with temperature. Therefore, according to Equation 6, properties such as the E_f modulus of elasticity, the Poisson ratio ν_f , the thermal expansion coefficient α_f , and the thermal conductivity coefficient K_f could be related to the temperature [1].

$$P_f(Z, T) = [P_c(T) - P_m(T)] \left(\frac{2Z+h}{2h} \right)^N + P_m(T) \quad (5)$$

2.2. The Fundamental Equation of FGM Plate

2.2.1. Displacement components

According to the classical theory of plates, the displacement field is as follows [21]:

$$\begin{aligned} u &= u_0(x, y, t) - z \bar{\psi}_x(x, y, t) \\ v &= v_0(x, y, t) - z \bar{\psi}_y(x, y, t) \quad , \quad w = w_0(x, y, t) \end{aligned} \quad (6)$$

In the above relations u_0 and v_0 , respectively, represent the displacements of the middle surface in the x and y directions, and w_0 is the transverse displacement along the z direction. Also, the functions $\bar{\psi}_x$ and $\bar{\psi}_y$ are rotations of the middle surface around x and y axes, respectively, and are as follows:

$$\bar{\psi}_x = \frac{\partial w_0}{\partial x} \quad , \quad \bar{\psi}_y = \frac{\partial w_0}{\partial y} \quad (7)$$

2.2.2. Nonlinear strain- displacement relations

The nonlinear relations of Von-Karman between strain and displacement at any point in the thickness of the plate at distance z from the middle surface according to

the strains and curvatures of the middle surface are as follows [22]:

$$\begin{aligned} \varepsilon_{xx} &= \varepsilon_{xx}^0 + Z\kappa_x & , & & \varepsilon_{yy} &= \varepsilon_{yy}^0 + Z\kappa_y \\ \gamma_{xy} &= \gamma_{xy}^0 + Z\kappa_{xy} & , & & \varepsilon_{zz} &= \varepsilon_{xz} = \varepsilon_{yz} = 0 \end{aligned} \quad (8)$$

In the above relations ε_{xx}^0 , ε_{yy}^0 and γ_{xy}^0 , are the strain of the middle surface and κ_x , κ_y and κ_{xy} are the curvatures of the middle surface, which are related to the displacement components u, v, w as follows:

$$\begin{aligned} \varepsilon_{xx}^0 &= \frac{\partial u}{\partial x} + \frac{1}{2} \left(\frac{\partial w}{\partial x} \right)^2 & , & & \varepsilon_{yy}^0 &= \frac{\partial v}{\partial y} + \frac{1}{2} \left(\frac{\partial w}{\partial y} \right)^2 \\ \gamma_{xy}^0 &= \frac{\partial u}{\partial y} + \frac{\partial v}{\partial x} + \frac{\partial w}{\partial x} \frac{\partial w}{\partial y} & , & & \kappa_x &= -\frac{\partial \psi_x}{\partial x} = -\frac{\partial^2 w}{\partial x^2} \\ \kappa_y &= -\frac{\partial \psi_y}{\partial y} = -\frac{\partial^2 w}{\partial y^2} & , & & \kappa_{xy} &= -\frac{\partial \psi_x}{\partial y} - \frac{\partial \psi_y}{\partial x} = -2 \frac{\partial^2 w}{\partial x \partial y} \end{aligned} \quad (9)$$

According to Hooke's law, the stress-strain relations are defined by the following Equation:

$$\begin{aligned} \begin{bmatrix} \sigma_{xx} \\ \sigma_{yy} \\ \sigma_{xy} \end{bmatrix} &= \begin{bmatrix} Q_{11} & Q_{12} & 0 \\ Q_{12} & Q_{22} & 0 \\ 0 & 0 & Q_{66} \end{bmatrix} \begin{bmatrix} \varepsilon_{xx} - \alpha(z, T) \Delta T \\ \varepsilon_{yy} - \alpha(z, T) \Delta T \\ \gamma_{xy} \end{bmatrix} \\ \sigma_{zz} &= \sigma_{xz} = \sigma_{yz} = 0 \end{aligned} \quad (10)$$

In the above relations, which include mechanical and thermal strains, α is the thermal expansion coefficient and Q_{ij} are the elements of the stiffness matrix, which are functions of the plate thickness and temperature; their relations are as follows:

$$\begin{aligned} Q_{11} = Q_{22} &= \frac{E_f(z, T)}{1 - \nu_f^2(T)} & , & & Q_{12} &= \frac{\nu_f E_f(z, T)}{1 - \nu_f^2(T)} \\ Q_{66} &= \frac{E_f(z, T)}{2(1 + \nu_f(T))} \end{aligned} \quad (11)$$

2.2.3. The Force and moment resultants

The vector of forces N and moments M caused by stresses in unit length are expressed in terms of strain components as follows [21]:

$$\begin{bmatrix} N_{xx} \\ N_{yy} \\ N_{xy} \end{bmatrix} = \int_{-h/2}^{h/2} \begin{bmatrix} \sigma_{xx} \\ \sigma_{yy} \\ \sigma_{xy} \end{bmatrix} dz & , & \begin{bmatrix} M_{xx} \\ M_{yy} \\ M_{xy} \end{bmatrix} = \int_{-h/2}^{h/2} \begin{bmatrix} \sigma_{xx} \\ \sigma_{yy} \\ \sigma_{xy} \end{bmatrix} z dz \quad (12)$$

By replacing stress relations from the above Equations, we can find the forces and moment resultants in terms of the following matrix strain:

$$\begin{Bmatrix} N - N^T \\ M - M^T \end{Bmatrix}_{6 \times 1} = \begin{bmatrix} [A] & [B] \\ [B] & [D] \end{bmatrix}_{6 \times 6} \begin{Bmatrix} \varepsilon^0 \\ k \end{Bmatrix}_{6 \times 1} \quad (13)$$

In the above relations N^T and M^T , are the thermal forces and moments resultants, matrices A, B, and D are the extensional, coupling, and bending stiffness matrices, respectively, and they are as follows:

$$\begin{aligned} [(A_{11}, A_{22}), (B_{11}, B_{22}), (D_{11}, D_{22})] &= \frac{1}{1 - \nu^2} (E_1, E_2, E_3) \\ (A_{12}, B_{12}, D_{12}) &= \frac{\nu}{1 - \nu^2} (E_1, E_2, E_3) \\ (A_{66}, B_{66}, D_{66}) &= \frac{\nu}{2(1 + \nu)} (E_1, E_2, E_3) \end{aligned} \quad (14)$$

In the above relations, the values of E_1 , E_2 , and E_3 are based on Young's modulus E_m , E_{cm} , the thickness of plate (h), and volumetric percentage index (N) for two cases of FGM plate (symmetric and asymmetric) as follows [5-6]:

Asymmetric

$$\begin{aligned} E_1 &= E_m h + \left(\frac{E_{cm} h}{N + 1} \right) \\ E_2 &= E_{cm} h^2 \left[\frac{1}{(N + 2)} - \frac{1}{(2N + 2)} \right] \\ E_3 &= \frac{E_m h^3}{12} + E_{cm} h^3 \left[\frac{1}{(N + 3)} - \frac{1}{(N + 2)} + \frac{1}{(4N + 4)} \right] \end{aligned} \quad (15)$$

Symmetric

$$\begin{aligned} E_1 &= E_{cm} h \left(1 + \frac{1}{N + 1} \right) & , & & E_2 &= 0 \\ E_3 &= E_{cm} h^3 \left[\frac{1}{12} + \frac{1}{4(N + 3)} \right] \end{aligned} \quad (16)$$

Therefore, by replacing the stresses (Equation. (10)) and the strains (Equation (8)) and the effective Young's modulus in Equations (12), the resultant forces and moments are obtained as follows:

$$\begin{aligned} N_{xx} &= \frac{E_1}{1 - \nu^2} (\varepsilon_{xx}^0 + \nu \varepsilon_{yy}^0) \\ &+ \frac{E_2}{1 - \nu^2} (k_x + \nu k_y) \\ &- \frac{\phi_m}{1 - \nu} \end{aligned} \quad (17)$$

$$N_{yy} = \frac{E_1}{1-\nu^2} (\varepsilon_{yy}^0 + \nu \varepsilon_{xx}^0) + \frac{E_2}{1-\nu^2} (k_y + \nu k_x) - \frac{\phi_m}{1-\nu}$$

$$N_{xy} = \frac{E_1}{2(1+\nu)} \gamma_{xy}^0 + \frac{E_2}{1+\nu} k_{xy}$$

$$M_{xx} = \frac{E_2}{1-\nu^2} (\varepsilon_{xx}^0 + \nu \varepsilon_{yy}^0) + \frac{E_3}{1-\nu^2} (k_x + \nu k_y) - \frac{\phi_b}{1-\nu}$$

$$M_{yy} = \frac{E_2}{1-\nu^2} (\varepsilon_{yy}^0 + \nu \varepsilon_{xx}^0) + \frac{E_3}{1-\nu^2} (k_y + \nu k_x) - \frac{\phi_b}{1-\nu}$$

$$M_{xy} = \frac{E_2}{2(1+\nu)} \gamma_{xy}^0 + \frac{E_3}{1+\nu} k_{xy}$$

In the above relations, the parameters ϕ_m and ϕ_b are as follows:

$$(\phi_m, \phi_b) = \int_{-h/2}^{+h/2} \left[E_m + E_{cm} \left(\frac{2z+h}{2h} \right)^N \right] \left[\alpha_m + \alpha_{cm} \left(\frac{2z+h}{2h} \right)^N \right] \Delta T(1, z) dz \quad (18)$$

Also, the thermal force and moment resultants (N^T and M^T) are defined as follows:

$$\begin{bmatrix} N_{xx}^T & M_{xx}^T \\ N_{yy}^T & M_{yy}^T \\ N_{xy}^T & M_{xy}^T \end{bmatrix} = - \int_{-h/2}^{+h/2} \begin{bmatrix} Q_{11} & Q_{12} & 0 \\ Q_{12} & Q_{22} & 0 \\ 0 & 0 & Q_{66} \end{bmatrix} \begin{bmatrix} 1 & 0 \\ 0 & 1 \\ 0 & 0 \end{bmatrix} \begin{bmatrix} \alpha(z, T) \\ \alpha(z, T) \end{bmatrix} \Delta T(1, z) dz \quad (19)$$

Where, ΔT is the increase of temperature relative to the reference temperature T_0 (without thermal strain) is as follows:

$$\Delta T = T(z) - T_0 \quad (20)$$

2.3. Equations of Motion of the Plate

The dynamic Equations of motion of the plate and its boundary conditions are extracted from Hamilton's principle, which are defined as four boundary conditions at the edges of the plate and three equilibrium Equations as follows [1], [6]:

$$\frac{\partial N_{xx}}{\partial x} + \frac{\partial N_{xy}}{\partial y} = 0, \quad \frac{\partial N_{yy}}{\partial y} + \frac{\partial N_{xy}}{\partial x} = 0$$

$$\frac{\partial^2 M_{xx}}{\partial x^2} + 2 \frac{\partial^2 M_{xy}}{\partial x \partial y} + \frac{\partial^2 M_{yy}}{\partial y^2} + N_{xx} \frac{\partial^2 w_0}{\partial x^2} + 2N_{xy} \frac{\partial^2 w_0}{\partial x \partial y} + N_{yy} \frac{\partial^2 w_0}{\partial y^2} + P - 2\mu \dot{w}_0 = I_0 \ddot{w}_0 \quad (21)$$

Where, $P(x, y, t)$ is the distribution of external force on the upper surface of the plate ($z = +h/2$) and μ is the coefficient of viscous damping per unit area of the plate. Also, I_0 is the inertial of the plate in the z -direction, and is defined as follows:

$$I_0 = \int_{-h/2}^{+h/2} \rho(z) dz \quad (22)$$

Where $\rho(z)$ is the density of the plate.

2.4. Boundary Condition

The boundary condition of the plate is defined as follows:

At $x=0$ and $x=L1$:

$$w_0 = v_0 = M_{xx} = 0, \quad N_{xx} = N_{xx}^* = -N_{xx}^0 \quad (23)$$

At $y=0$ and $y=L2$:

$$w_0 = v_0 = M_{yy} = 0, \quad N_{yy} = N_{yy}^* = -N_{yy}^0 \quad (24)$$

2.5. Extraction of The Equation of FGM Plate Deflection

In order to establish the first two Equations of motion (Equations (21)), the function of the potential stress field ϕ is considered as follows [6]:

$$N_{xx} = \phi_{,yy}, \quad N_{yy} = \phi_{,xx}, \quad N_{xy} = -\phi_{,xy} \quad (25)$$

Moreover, the third Equation (Equation (21)) can be obtained in terms of the two unknown parameters of the stress field (ϕ) and the transverse displacement (w_0). For this purpose, by applying inverse algebraic operations on Equation (13), it can be written as follows:

$$\begin{Bmatrix} \{\varepsilon^0\} \\ \{M\} - \{M^T\} \end{Bmatrix} = \begin{bmatrix} [A^*] & [B^*] \\ -[B^*]^T & [D^*] \end{bmatrix} \begin{Bmatrix} \{N\} - \{N^T\} \\ \kappa \end{Bmatrix} \quad (26)$$

As shown in Equation 26, the matrices shown are as follows:

$$[A^*] = [A]^{-1}, \quad [B^*] = -[A]^{-1}[B]$$

$$[B^*]^T = -[B][A]^{-1}, \quad [D^*] = [D] - [B][A]^{-1}[B] \quad (27)$$

By substituting the above relations, in the third Equation of motion of the plate and simplifying, the first fourth-order governing Equation is obtained with respect to two unknown parameters of the stress field (ϕ) and transverse displacement (w_0) [6]:

$$D \nabla^4 w_0 - (\phi_{,xx} w_{0,yy} - 2\phi_{,xy} w_{0,xy} + \phi_{,yy} w_{0,xx}) + I_0 \ddot{w}_0 + 2c \dot{w}_0 = P - \left(\frac{E_2}{E_1} \right) \nabla^2 N^T + \nabla^2 M^T \quad (28)$$

Where, D is a parameter defined as follows:

$$D = \frac{E_1 E_3 - E_2^2}{E_1 (1 - \nu^2)} \quad (29)$$

To solve the above Equation, we need another Equation including two unknown parameters mentioned above, which can be obtained from the compatibility conditions and simplification. The compatibility Equation is:

$$\begin{aligned} &\varepsilon_{xx,yy} + \varepsilon_{yy,xx} \\ &- \gamma_{xy,xy} \\ &= w_{,0,xy}^2 \\ &- w_{,0,xx} w_{,0,yy} \end{aligned} \quad (33)$$

By substituting the strains from relation 17 and the function field of stress potential (relations 25) in Equation (30), the second fourth-order governing Equation, including two unknown parameters of the stress field (ϕ) and the transverse displacement (w_0) is obtained as follows:

$$\nabla^4 \phi = E_1 (w_{0,xy} - w_{0,xx} w_{0,yy}) - (1 - \nu) \nabla^2 N^T \quad (31)$$

Thus, two Equations 28 and 31 are the basic governing Equations, including the terms of thermal force and moment resultants to obtain the general dynamic response of the FGM plates under the external excitation.

3 SOLVING EQUATION OF FGM PLATES BY CONSIDERING THERMAL TERMS

In order to solve the governing Equations in general, taking into account the boundary conditions, the unknown parameters of w_0 and ϕ are assumed to be in the form of sinusoid functions as follows [6]:

$$w_0(x, y, t) = w_{mn}(t). \sin \lambda_m x. \sin \mu_n y \quad (32)$$

$$\begin{aligned} \phi(x, y, t) = &A_{mn}(t) \cos 2\lambda_m x + B_{mn}(t) \cos 2\mu_n y + \\ &C_{mn}(t) \cos 2\lambda_m x \cos 2\mu_n y + D_{mn}(t) \sin \lambda_m x \sin \mu_n y \\ &+ \frac{1}{2} N_{xx}^* y^2 + \frac{1}{2} N_{yy}^* x^2 \end{aligned} \quad (33)$$

Where:

$$\mu_n = \frac{n\pi}{L_2}, \quad \lambda_m = \frac{m\pi}{L_1} \quad (34)$$

In Equation (32), $w_{mn}(t)$ is the maximum deflection of the FGM plates, and $m, n = 1, 2, 3, \dots$, represent the number of half waves along the axes x and y , respectively.

Also, thermal force and moment resultants are assumed to be in the form of the following functions:

$$\begin{aligned} N^T &= N_{mn}^T \sin \lambda_m x \sin \mu_n y \\ M^T &= M_{mn}^T \sin \lambda_m x \sin \mu_n y \end{aligned} \quad (35)$$

Where, N_{mn}^T and M_{mn}^T from relation 19 are obtained as follows:

$$\begin{aligned} N_{xx}^T &= N_{yy}^T \\ &= \frac{h \Delta T}{1 - \nu(T)} \left[\frac{E_{cm}(T) \alpha_{cm}(T)}{2N + 1} \right. \\ &+ \frac{E_{cm}(T) \alpha_{cm}(T) + E_m(T) \alpha_{cm}(T)}{N + 1} \\ &+ \left. E_m(T) \alpha_m(T) \right] \end{aligned} \quad (36)$$

$$\begin{aligned} M_{xx}^T = M_{yy}^T = &-\frac{h^2 \Delta T}{1 - \nu(T)} \left\{ E_{cm}(T) \alpha_{cm}(T) \left(\frac{1}{2N + 2} - \right. \right. \\ &\left. \frac{1}{4N + 2} \right) + E_{cm}(T) \alpha_m(T) \left(\frac{1}{N + 2} - \frac{1}{2N + 2} \right) \\ &+ \left. E_m(T) \alpha_{cm}(T) \left(\frac{1}{N + 1} - \frac{1}{2N + 2} \right) \right\} \end{aligned} \quad (37)$$

$$N_{xy}^T = M_{xy}^T = 0$$

By substituting Equation (32), (33) and (35) into (31), the coefficients of A_{mn} , B_{mn} , C_{mn} and D_{mn} are obtained as follows:

$$\begin{aligned} A_{mn}(t) &= \frac{E_1 w_{mn}^2(t) \mu_n^2}{32 \lambda_m^2}, \quad B_{mn}(t) = \frac{E_1 w_{mn}^2(t) \lambda_m^2}{32 \mu_n^2} \\ C_{mn}(t) &= 0, \quad D_{mn}(t) = \frac{N_{mn}^T ((1 - \nu))}{(\lambda_m^2 + \mu_n^2)} \end{aligned} \quad (38)$$

Therefore, by replacing these coefficients in relation 33, the function ϕ is obtained as follows:

$$\begin{aligned} \phi(x, y, t) = & \frac{E_1 W_{mn}^2(t) \mu_n^2}{32 \lambda_m^2} \cos 2 \lambda_m x + \frac{E_1 W_{mn}^2(t) \lambda_m^2}{32 \mu_n^2} \\ & \cos 2 \mu_n y + \frac{N_{mn}^T (1-\nu)}{(\lambda_m^2 + \mu_n^2)} \sin \lambda_m x \sin \mu_n y + \\ & \frac{1}{2} N_{xx}^* y^2 + \frac{1}{2} N_{yy}^* x^2 \end{aligned} \quad (39)$$

The external excitation force on the plate is considered to be proportional to the transverse displacement as follows:

$$P_t(x, y, t) = P_{mn}(t) \sin \lambda_m x \sin \mu_n y \quad (40)$$

In the above relation, the coefficient $P_{mn}(t)$ is obtained by the Fourier series expansion as follows:

$$P_{mn}(t) = \frac{4}{L_1 L_2} \int_0^{L_1} \int_0^{L_2} P_t(x, y, t) \sin \lambda_m x \sin \mu_n y dx dy \quad (41)$$

In this research, the external load applied on the FGM plate is explosive load and the type of the explosive loading is considered as a free in-air spherical air burst. Such an explosion creates a spherical shock wave that travels radially outward in all directions with diminishing velocity. The form of the incident blast wave from a spherical charge is shown in "Fig. 2".

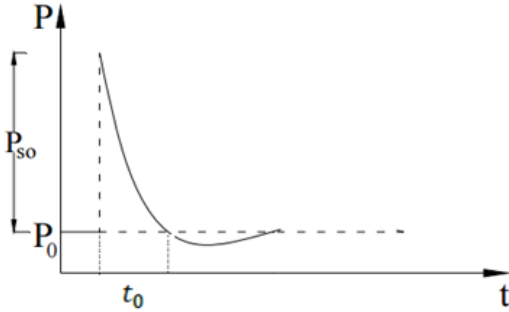


Fig. 2 Incident pressure profile of a blast wave [23].

Where P_{s0} is the peak overpressure above ambient pressure, P_0 is the ambient pressure, t_a is the time of arrival, t_p is the positive phase duration of the blast wave, t is the time and b is the coefficient of reduction of the amplitude wave of the explosion which is determined by adjustment to a pressure curve from a blast test. The waveform shown in "Fig. 2" is given by an expression known as the Friedlander Equation and is given as follows [6], [23]:

$$P_t(t) = (P_{s0} - P_0) \left(1 - \frac{(t - t_a)}{t_p} \right) \exp \left(-b \frac{(t - t_a)}{t_p} \right) \quad (42)$$

Where

$$P_{s0} = 172/Z^3 - 114/Z^2 + 108/Z, \quad Z = R/W^{1/3}$$

Where, R is the standoff distance in meters and W is the equivalent charge weight of TNT in kilograms. By substituting Equation (42) in (41), $P_{mn}(t)$ under the loading due to the explosion, it is obtained as follows:

$$P_{mn}(t) = \frac{16P_t(t)}{\pi^2}, \quad (m, n) = (1, 1) \quad (43)$$

By replacing Equation (39) and (32) in (28), and using the Galerkin method, the following second-order Equation describing the nonlinear differential governing Equations of FGM plates under external excitation due to the explosion considering the expressions of the thermal force and moment resultants are obtained. The main unknown parameter of these Equations is the $W_{mn}(t)$ plate, which is the purpose of this research obtained as follows:

$$\begin{aligned} \ddot{w}_{mn}(t) + \frac{2c}{I_0} \dot{w}_{mn}(t) + \omega_{mn}^2 w_{mn}(t) + \\ \frac{E_1 (\lambda_m^4 L_2 + \mu_n^4 L_1)}{16I_0} w_{mn}^3(t) = \\ \frac{1}{I_0} \left(P_{mn}(t) + (\lambda_m^2 + \mu_n^2) \left(\frac{E_2}{E_1} N_{mn}^T - M_{mn}^T \right) \right) \end{aligned} \quad (44)$$

In Equation (44), $w_{mn}(t)$ is the deflection of the FGM plate in terms of time, and the natural frequency ω_{mn} is obtained from the following Equation:

$$\omega_{mn} = \sqrt{\frac{K_{mn}}{I_0}} \quad (45)$$

I_0 is the mass moment-of-inertia of the plate and the K_{mn} is defined as follows:

$$\begin{aligned} K_{mn} = \frac{(E_1 E_3 - E_2^2) \pi^4}{E_1 L_1^4 (1-\nu^2)} (m^4 + 2m^2 n^2 \psi^2 + n^4 \psi^4) + \\ \left(N_{xx}^* \frac{m^2 \pi^2}{L_1^2} + N_{yy}^* \frac{n^2 \pi^2}{L_2^2} \right) \end{aligned} \quad (46)$$

Where, ψ is the ratio of length to width of the plate (aspect ratio). Also, in Equation (44) the dimensionless damping coefficient Δ_{mn} could be defined as follows:

$$\frac{2}{I_0} \mu = 2\Delta_{mn} \omega_{mn} \rightarrow \Delta_{mn} = \frac{\mu}{I_0 \omega_{mn}} \quad (47)$$

In order to obtain a time response of FGM plate, the fourth-order Ronge-Kutta code with zero initial conditions in the MATLAB program is used to solve Equation (44) which is a second-order nonlinear non-homogeneous differential Equation.

4 RESULTS AND DISCUSSION

4.1. Validation

The considered FGM plate consists of Titanium alloy Ti-6Al-4V as a metal component and aluminum oxide as a ceramic component and has been restrained as simply supported on all edges. Its geometric and physical characteristics are selected in accordance with “Tables 1 and 2” [6]. Also, the number of half-waves considered along the axes x and y are $m = n = 1$, respectively.

Table 1 Geometric parameters of FGM plate

aspect ratio(ψ)	h (m)	L_2 (m)	L_1 (m)
1	0.0254	1	1

Table 2 Mechanical properties of FGM plate

E_m (GPa)	E_c (GPa)	ν_m	ν_c
105.7	320.24	0.2981	0.26
α_m ($^{\circ}\text{C}^{-1}$)	α_c ($^{\circ}\text{C}^{-1}$)	ρ_m ($\frac{kg}{m^3}$)	ρ_c ($\frac{kg}{m^3}$)
8.7×10^{-6}	7.1×10^{-6}	4429	3750

Also, the characteristics of the explosive loading wave in the air, the weight of the explosive, and distance of its center from the plate are shown in “Table 3”.

Table 3 Characteristics of the explosive wave loading

α	W (Kg)	R (m)	t_a (s)	T_p (s)
0.5	0.7	0.766	0.000408	0.001372

In order to verify the results, using the above Tables, in similar geometric conditions and similar loading, the results of this study are compared with the results of Ref. [6]. Time response of the center point deflection of FGM plate in terms of the explosion time without consideration of temperature mode for asymmetric and symmetrical states with a volumetric percentage index of $N = 0.5$ are shown in “Figs. 3 and 4”, respectively. Comparison between the results of Ref. [6] and the

present study have been presented in “Tables 4 and 5”. This comparison shows that the error percentage between them is negligible which confirms the accuracy of the present study.

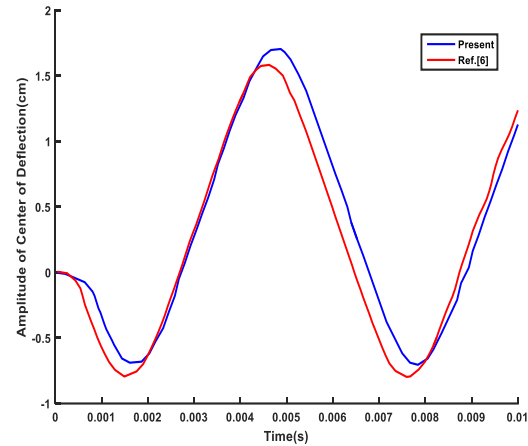


Fig. 3 Time response of the center point deflection of asymmetric FGM plate with $N=0.5$ without thermal effects.

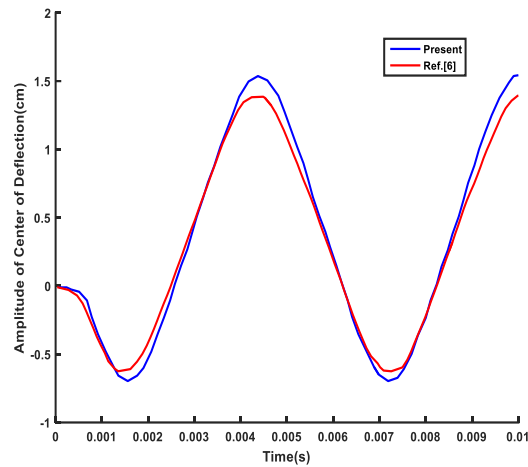


Fig. 4 Time response of the center point deflection of symmetric FGM plate with $N=0.5$ without thermal effects.

Table 4 Comparison between the results of Ref. [6] and the present study

Asymmetric FGM plate			
	Ref.[6]	Present study	Error
Maximum deflection in the first period(cm)	1.6	1.7	%6.25
Time of maximum deflection in the first period(s)	0.0046	0.0049	%6.5

Table 5 Comparison between the results of Ref. [6] and the present study

Symmetric FGM plate			
	Ref.[6]	Present study	Error
Maximum deflection in the first period(cm)	1.39	1.53	% 10
Time of maximum deflection in the first period(s)	0.0043	0.0044	%2.32

4.2. Effects of Different Parameters on The Dynamic Response

In this section, the results of the parametric study of the effect of different parameters on the time response of the center point deflection of the FGM plate have been investigated. The effect of temperatures $\Delta T(K) = (30,500,600, 700)$ on the nonlinear dynamic response of the asymmetric FGM plates with $N = 0.5$ is shown in “Fig. 5”. The geometrical and mechanical properties of the FGM plate and the characteristics of the explosive wave loading are similar to the previous ones. It can be seen that the dynamic response amplitude increases when the temperature ΔT increases since the flexibility of the plate increases. It means that the dynamic response amplitude is directly proportional to the temperature ΔT . The results of the first period in each temperature are given in “Table 6”.

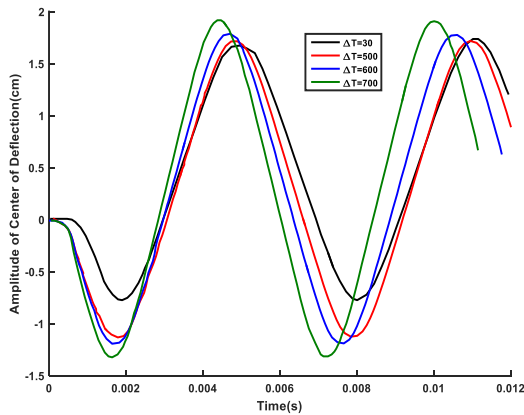


Fig. 5 The effect of temperature on the nonlinear response of the FGM plates under blast load with $N=0.5$.

Figure 6 shows the effect of the volumetric percentage index N on the nonlinear dynamic response of the asymmetric FGM plates with $N = 0, 5, 10, 50$ and considering the effect of thermal forces and moments resultants. Obviously, the amplitude of the nonlinear dynamic response of the FGM plate is directly proportional to the power-law index N . At $N = 0$, the plate has a pure ceramic property and by increasing N , the metal property is added. In fact, by increasing N , the

behavior of the plate becomes more flexible and the deflection is increased, as a result, the plate exhibits more geometric nonlinear effects.

Table 6 The effect of temperature on the response FGM plate

Results	Asymmetric FGM plate with $N=0.5$			
	Difference temperature ($^{\circ}C$)			
	700	600	500	25
Maximum deflection in the first period(cm)	1.92	1.79	1.71	1.67
The time of Maximum deflection in the first period(s)	0.0043	0.0047	0.0049	0.005

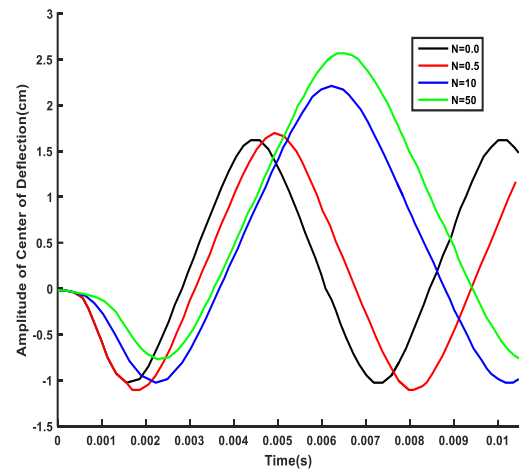


Fig. 6 The effect of power-law index N on the time response of the center point deflection of asymmetric FGM plate with $\Delta T = +600^{\circ}C$ and without damping effect under blast load.

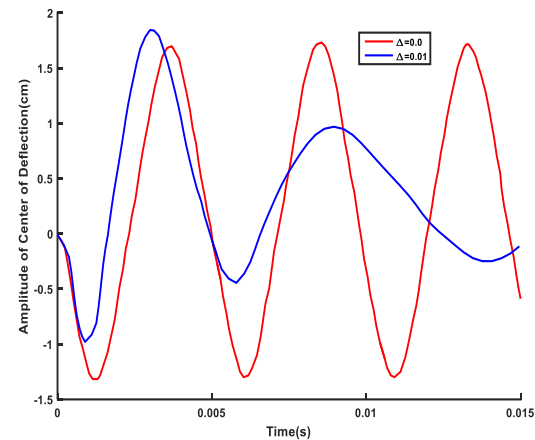


Fig. 7 The effect of various amounts of damping on the time response of the center point deflection of asymmetric FGM plate with $N=0.5$.

Effects of various amounts of damping on the time response of the center point deflection of asymmetric FGM plate with $N=0.5$ and without temperature are shown in “Fig. 7”. It can be seen that central deflections vs. time attenuate faster as the amount of the damping coefficient is increased for a fixed volume fraction of the constituent materials. Because damping causes waste of energy and reduces the deflection amplitude.

The effect of damping with a value of $\Delta 11 = 0.1$ on the time response of the center point deflection of symmetric and asymmetric FGM plate with $N=0.5$ is also compared with temperature ($\Delta T = +600\text{ }^\circ\text{C}$) and without temperature as shown in “Fig. 8”. As can be seen, regardless of the thermal effects, the smaller deflection amplitude corresponds to the symmetric FGM configuration.

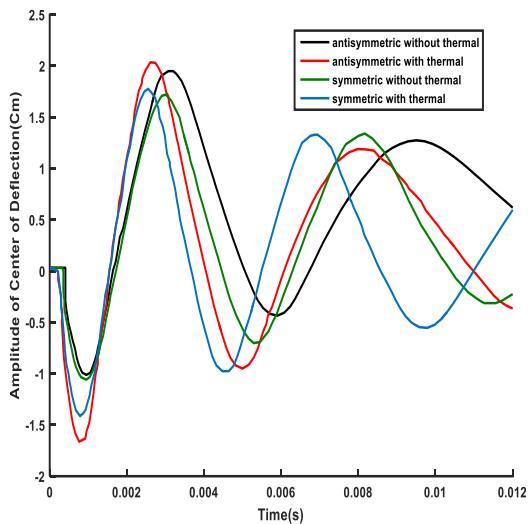


Fig. 8 The effect of FGM configuration on the time response of the center point deflection of symmetric and asymmetric FGM plate with temperature ($\Delta T = +600\text{ }^\circ\text{C}$) and without temperature.

Also, the effects of various amounts of damping on the time response of center point deflection of asymmetric FGM plate with $N=0.5$ and with temperature $\Delta T = +600\text{ }^\circ\text{C}$ are shown in “Fig. 9”. It can be seen that by increasing the amount of the damping coefficient, the amplitude of the central deflections vs. time is decreased and damped. Because damping causes a waste of energy and reduces deflection in the presence of thermal effect. Figure 10 illustrates the effect of the aspect ratio (L_1/L_2) of the plate on the time response of the center point deflection of the FGM plate under blast load with $N=0.5$. It is clear that the plate fluctuation amplitude decreases when increasing the aspect ratio of the plate. In conclusion, the plate fluctuation amplitude is in inverse proportion to the aspect ratio of the plate. So, in similar conditions, by doubling the ratio of length to width of

the plate ($\psi=2$), the center deflection of the plate is decreased by about 70%. Therefore, for optimal design, the use of FGM plates with a high aspect ratio leads to smaller deflections against blast load and consequently leads to lower stress values.

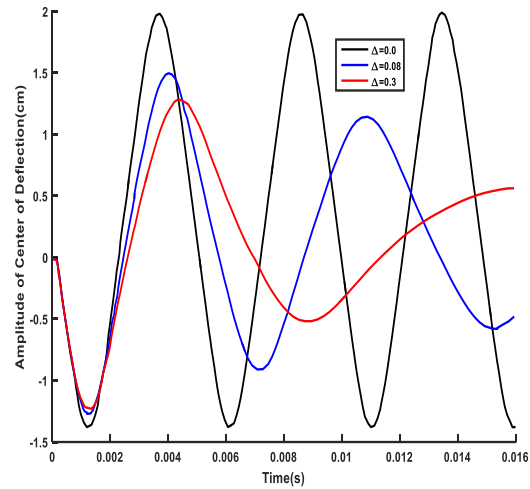


Fig. 9 The effect of various amounts of damping on the time response of the center point deflection of asymmetric FGM plate with $N=0.5$ and temperature ($\Delta T = +600\text{ }^\circ\text{C}$).

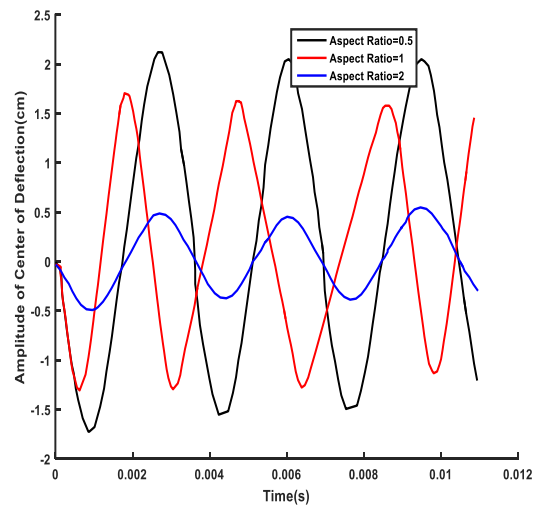


Fig. 10 The effect of aspect ratio (L_1/L_2) of asymmetric FGM plate on the time response of the center point deflection under blast load.

Figure 11 shows the effect of explosive mass on the time response of the center point deflection of FGM plate under blast load. The physical and geometric characteristics of the plate and the characteristics of the explosive loading are the same as in the previous cases, and only the explosive mass is different. As can be seen, the center point deflection amplitude of FGM plate

increases when explosive mass is increased. Amplitude of deflection is directly proportional to the explosive mass. For example, an increase in the mass of explosives from 0.4 to 0.7 kg leads to an increase in the central deflection of the plate at the peak of the first period from 1.41 cm to 1.69 cm, which is an increase of about 20%, as well as an increase the mass, reduces the occurrence time of the peak of the domain during the first period from 0.0056 seconds to 0.0044 seconds.

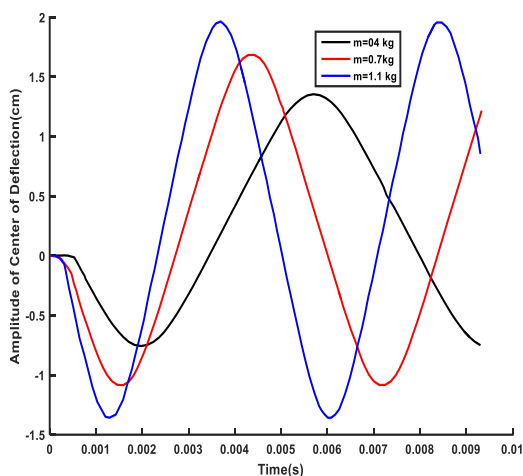


Fig. 11 The effect of explosive mass on the time response of the center point deflection of FGM plate under blast load with $N = 0.5$.

5 CONCLUSIONS

In this paper, the behavior and dynamic response of FGM plates against blast load were investigated. The main purpose of the reduction of deflection and displacement is to reduce the stresses caused by the explosion waves in the plates. Various factors and parameters are effective in increasing or decreasing the deflection of the plate, including the FGM material percentage index (N), the aspect ratio of the plate, the geometric structure of the FGM plate (phase gradation) in terms of the symmetrical or asymmetric structure, weight of the explosive, the distance of the explosive from the plate, the damping, the effects of temperature, etc. In the present study, these parameters were investigated. Finally, the following results can be summarized:

A) The amplitude of the center point deflection of the FGM plate is less than the pure metal plates when exposed to the blast load and in the FGM plates, the deformation of symmetrical plates is smaller than the asymmetric plates.

B) By applying the damping coefficient of the FGM plates, the amplitude of the center point deflection is reduced and damped during the explosion.

C) By increasing the aspect ratio of the FGM plate, its center point deflection against explosion waves reduces. Therefore, the use of plates with a high aspect ratio leads to smaller deflection and lower stress values.

D) By increasing the volumetric index percentage of FGM, the center point deflection is increased.

E) By considering the effects of thermal resultant forces and moments, the center point deflection is increased and by increasing the temperature, the center point deflection of the plate is increased.

Finally, it should be noted that the theory presented in this study is based on the theory of elasticity, and no plastic deformation or fracture is considered, and it is assumed that the behavior of the plate remains elastic all the time.

REFERENCES

- [1] Shen, H. S., *Functionally Graded Materials: Nonlinear Analysis of Plates and Shells*, CRC Press, Taylor & Francis Group, London, New York, Published January 15, 2011, ISBN 9780367386016.
- [2] Turkmen, H. S., Mecitoglu, Z., *Dynamic Response of a Stiffened Laminated Composite Plate Subjected to Blast Load*, *Journal of Sound and Vibration*, Vol. 221, No 3, 1999, pp. 371-389, DOI.org/10.1006/jsvi.1998.1976.
- [3] Chi, S., Chung, U., *Mechanical Behavior of Functionally Graded Material Plates Under Transverse Load*, *Int. J. Solids and Structures*, Vol. 43, NO. 13, 2006, pp. 3657-3674, DOI.org/10.1016/j.ijsolstr.2005.04.011.
- [4] Alibeigloo, A., *Exact solution for Thermoelastic Response of Functionally Graded Rectangular Plates*, *Composite Structures*, Vol. 92, No. 1, 2010, pp. 113-121, DOI.org/10.1016/j.compstruct.2009.07.003.
- [5] Tung, H. V., Duc, N. D., *Nonlinear Analysis of Stability for Functionally Graded Plates Under Mechanical and Thermal Loads*, *Composite Structures*, Vol. 92, No. 5, 2010, pp. 1184-1191, DOI.org/10.1016/j.compstruct.2009.10.015.
- [6] Hause, T., *Advanced Functionally Graded Plate-Type Structures Impacted by Blast Loading*, *International Journal of Impact Engineering*, Vol. 38, No. 5, 2011, pp. 314-321, DOI.org/10.1016/j.ijimpeng.2010.11.006.
- [7] Aksoylar, C., Ömercikog̃lu, A., Mecitog̃lu, Z., and Omurtag, M. H., *Nonlinear Transient Analysis of Fgm and FML Plates Under Blast Loads*, *Composite Structures*, Vol. 94, No. 2, 2012, pp. 731-744, DOI.org/10.1016/j.compstruct.2011.09.008.
- [8] Sreenivas, P., Siva Kumar, A., Pavuluri, S., and Kumari, A. A., *Investigation on Transient Dynamic Response of Functionally Graded Materials*, *International Journal of Application or Innovation in Engineering & Management*, Vol. 2, No. 9, 2013, pp. 214-218.
- [9] Goudarzi, M., Zamani, J., *Experimental and Numerical Investigation of the Maximum Deflection of Circular Aluminum Plate Subjected to Free Air Explosion*, (In

- Persian) Modares Mechanical Engineering, Vol. 15, No. 1, 2015, pp. 219-226.
- [10] Duong, N. T., Duc, N. D., Evaluation of Elastic Properties and Thermal Expansion Coefficient of Composites Reinforced by Randomly Distributed Spherical Particles with Negative Poissons Ratio, Composite Structures, Vol. 153, 2016, pp. 569–577, DOI:10.1016/j.compstruct.2016.06.069.
- [11] Duc, N. D., Duc, N., Tuan, N. D., Tran, P., and Quan, T. Q., Nonlinear Dynamic Response and Vibration of Imperfect Shear Deformable Functionally Graded Plates Subjected to Blast And Thermal Load, Journal of Mechanics of Advanced Materials and Structure, Vol. 24, No. 4, 2016, pp. 318-329, DOI:10.1080/15376494.2016.1142024.
- [12] Duc, N. D., Quang, V. D., and Anh, V. T. T., The Nonlinear Dynamic and Vibration of the S-FGM Shallow Spherical Shells Resting On an Elastic Foundations Including Temperature Effects, International Journal of Mechanical Sciences, Vol. 123, 2017, pp. 54–63, DOI.org/10.1016/j.ijmeosci.2017.01.043.
- [13] Cong, P. H., Anh, V. M., and Duc, N. D., Nonlinear Dynamic Response of Eccentrically Stiffened FGM Plate using Reddys TSDT in Thermal Environment, Journal of Thermal Stresses, Vol. 40, No. 6, 2017, pp. 704–732, DOI.org/10.1080/01495739.2016.1261614.
- [14] Hajlaoui, A., Triki, E., Frikha, A., Wali, M., and Dammak, F., Nonlinear Dynamics Analysis of FGM Shell Structures with a Higher Order Shear Strain Enhanced Solid-Shell Element, Latin American Journal of Solids and Structure, Vol. 14, 2017, pp. 72-91, DOI.org/10.1590/1679-78253323.
- [15] Thang, P. T., Duc, N. D., and Nguyen-Thoi, T., Thermomechanical Buckling And Post-Buckling of Cylindrical Shell with Functionally Graded Coatings and Reinforced by Stringers, Aerospace Science and Technology, Vol. 66, 2017, pp. 392-401, DOI.org/10.1016/j.ast.2017.03.023.
- [16] Duc, N. D., Quang, V. D., Nguyen, P. D., and Chien, T. M., Nonlinear Dynamic Response of Functionally Graded Porous Plates on Elastic Foundation Subjected to Thermal and Mechanical Loads, J. Appl. Comput. Mech., Vol. 4, No. 4, 2018, pp. 245-259, DoI:10.22055/JACM.2018.23219.1151.
- [17] Hong kong, P., Dinh Duc, N., Studied Analytical Solutions for The Nonlinear Dynamic Response of ES-FGM Plate Under Blast Load, Vietnam Journal of Mechanics, VAST, Vol. 40, No. 1, 2018, pp. 33 – 45, DOI:10.15625/0866-7136/9840.
- [18] Kim, S. E., Duc, N. D., Nam, V. H. and Sy, N. V., Nonlinear Vibration and Dynamic Buckling of Eccentrically Oblique Stiffened FGM Plates Resting On Elastic Foundations in Thermal Environment, Thin-Walled Structures, Vol. 142, 2019, pp. 287-296, DOI.org/10.1016/j.tws.2019.05.013.
- [19] Duc, N. D., Hadavinia, H., Quan, T. Q., and Khoa, N. D., Free Vibration and Nonlinear Dynamic Response of Imperfect Nanocomposite FG-CNTRC Double Curved Shallow Shells in Thermal Environment, European Journal of Mechanics - A/Solids, Vol. 75, 2019, pp. 355-366, DOI.org/10.1016/j.euromechsol.2019.01.024.
- [20] Upadhyay, A., Shukla, K., Geometrically Nonlinear Static and Dynamic Analysis of Functionally Graded Skew Plates, Communication in Nonlinear Science and Numerical Simulation, Vol. 18, No. 8, 2013, pp. 2252-2279, DOI.org/10.1016/j.cnsns.2012.12.034.
- [21] Soltani, M., Hatami, S., and Azhari, M., Free Vibration of Thin Functionally Graded Plates by Exact Finite Strip Method, Journal of computational Methods in Engineering, Vol. 32, No. 2, 2014, pp. 33-54.
- [22] Thang, P. T., Nguyen-Thoi, T., and Lee, J., Closed-form Expression for Nonlinear Analysis of Imperfect Sigmoid-FGM Plates with Variable Thickness Resting On Elastic Medium, Composite Structures, Vol. 143, 2016, pp. 143-150, DOI.org/10.1016/j.compstruct.2016.02.002.
- [23] Smith, P., Hetherington, J., Blast and Ballistic Loading of Structures, 1st Edition, CRC Press. Tylor & Francis GrouPublished August 15, 1994, ISBN 9780367866877.